


Anti-cryptococcal activity of preussolides A and B, phosphoethanolamine-substituted 24-membered macrolides, and leptosin C from coprophilous isolates of *Preussia typharum*

Bruno Perlatti¹, Nan Lan¹, Meichun Xiang², Cody E. Earp³, Joseph E. Spraker⁴, Colin J. B. Harvey⁴, Connie B. Nichols⁵, J. Andrew Alspaugh ⁵, James B. Gloer ³, Gerald F. Bills ¹

¹Texas Therapeutics Institute, The Brown Foundation Institute of Molecular Medicine, University of Texas Health Science Center at Houston, Houston, TX 77054, USA

²State Key Laboratory of Mycology, Institute of Microbiology, Chinese Academy of Sciences, No. 3 Park 1, Beichen West Road, Chaoyang District, Beijing 100101, China

³Department of Chemistry, University of Iowa, Iowa City, IA 52242, USA

⁴Hexagon Bio, Menlo Park, CA 94025, USA

⁵Departments of Medicine and Molecular Genetics & Microbiology, Duke University Medical Center, Durham, NC 27710, USA

Correspondence should be addressed to: Gerald F. Bills at billsge@vt.edu

Abstract: *Cryptococcus neoformans* is a serious human pathogen with limited options for treatment. We have interrogated extracts from fungal fermentations to find *Cryptococcus*-inhibiting natural products using assays for growth inhibition and differential thermosensitivity. Extracts from fermentations of four fungal strains from wild and domestic animal dung from Arkansas and West Virginia, USA were identified as *Preussia typharum*. The extracts exhibited two antifungal regions. Purification of one region yielded new 24-carbon macrolides incorporating both a phosphoethanolamine unit and a bridging tetrahydrofuran ring. The structures of these metabolites were established mainly by analysis of high-resolution mass spectrometry and 2D NMR data. Relative configurations were assigned using NOESY data, and the structure assignments were supported by NMR comparison with similar compounds. These new metabolites are designated preussolides A and B. The second active region was caused by the cytotoxin, leptosin C. Genome sequencing of the four strains revealed biosynthetic gene clusters consistent with those known to encode phosphoethanolamine-bearing polyketide macrolides and the biosynthesis of dimeric epipolythiodioxopiperazines. All three compounds showed moderate to potent and selective antifungal activity toward the pathogenic yeast *C. neoformans*.

Keywords: Antifungal, *Cryptococcus*, Ethanolamine phosphate transferase, Epipolythiodioxopiperazine, Polyketides, Sporormiaceae

Introduction

Cryptococcus neoformans and *C. gatii* are basidiomycete yeasts found in many varied regions of the world. These species are frequent opportunistic pathogens in highly immunocompromised patients, especially those with late-stage HIV infection. Given their ability to remain clinically dormant after initial infection, these fungal pathogens can re-emerge from latently infected sites in the setting of impaired CD4-mediated immunity, most often resulting in lethal infections of the central nervous system (Rajasingham et al., 2017). Although many immunosuppressed populations are at risk for infections due to *Cryptococcus* species, there were an estimated 220 000 annual cases of *C. neoformans* infections in 2017 worldwide, and up to a 75% mortality rate, specifically in patients with AIDS (Bongomin et al., 2017; Rajasingham et al., 2017). Treatment routinely depends on decades-old antifungal agents (azoles, amphotericin B, flucytosine) that are associated with poor outcomes due to high toxicity, elevated recurrence rates, the need for long-term suppressive therapy, and emergence of drug resistance (Brown et al., 2012; Perfect, 2017). In part, these drawbacks can be associated with the fact that antifungal compounds identified by whole-cell screening have generally

targeted pathogenic fungi other than *Cryptococcus*, especially the ascomycetes *Candida albicans* and *Aspergillus fumigatus*. Therefore, targeting the basidiomycete *C. neoformans* for discovery of new antifungal agents could reveal overlooked molecules with potential as novel drug candidates (Butts et al., 2013; Krysan, 2015).

Among strategies and techniques for discovery of antifungal agents, fungal metabolites represent a rich source of intrinsically antifungal molecules with one of the highest probabilities for success due to the likelihood for their interaction with fungal-specific targets (Roemer et al., 2011). Dung-inhabiting fungi, also known as coprophilous fungi, are a specialized ecological assemblage of fungi adapted to colonize, decompose, and reproduce in animal dung (Dix & Webster, 1995; Doveri, 2004). They often exhibit traits that aid in gaining access to and completing their life cycle in the dung habitat, including rapid reproduction, forcibly discharged spores or sporangia that stick to plant surfaces, homothallic mating systems, and strong enzyme systems for degradation of plant polymers (Dix & Webster, 1995). There is some evidence that certain species need passage through the gut to activate spore germination, although, they are thought not to be active in the internal gut microbiome. However, once dung is deposited, members of the coprophilous assemblage quickly

Received: November 17, 2020. Accepted: February 13, 2021.

© The Author(s) 2021. Published by Oxford University Press on behalf of Society of Industrial Microbiology and Biotechnology. This is an Open Access article distributed under the terms of the Creative Commons Attribution-NonCommercial-NoDerivs licence (<http://creativecommons.org/licenses/by-nc-nd/4.0/>), which permits non-commercial reproduction and distribution of the work, in any medium, provided the original work is not altered or transformed in any way, and that the work is properly cited. For commercial re-use, please contact journals.permissions@oup.com

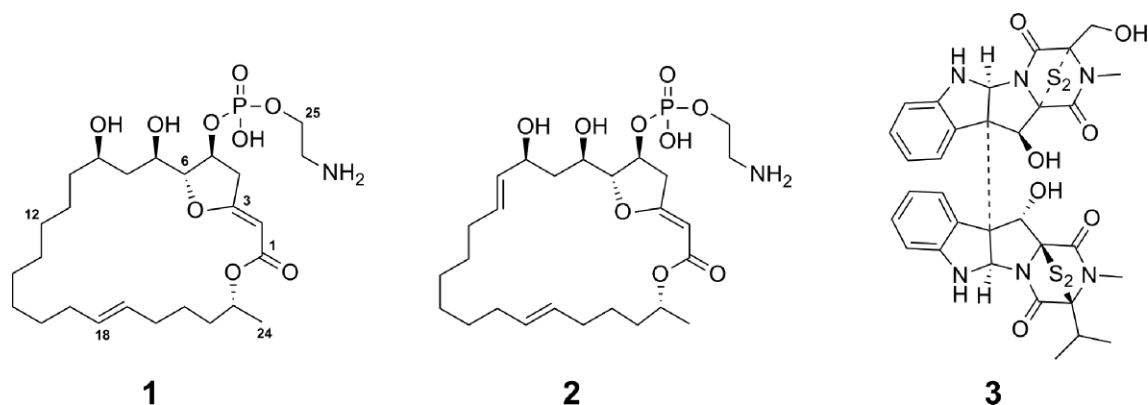


Fig. 1 Compounds 1–3 isolated from strains of *Preussia typharum* from Arkansas and West Virginia, USA.

colonize and reproduce on the dung in a predictable succession (Richardson, 2002; Wicklow, 1992). It has been observed that the later-stage species tend to be filamentous ascomycetes of the Dothidiomycetes, Sordariomycetes, and Eurotiomycetes, and that these fungi maybe highly antagonistic to other fungi, arthropods, and nematodes, thus securing their places in the late succession. At least in part this antagonistic behavior is mediated by their rich secondary metabolism (Wicklow, 1981, 1988; Wicklow & Hirschfield, 1979). Thus, they are readily accessible microbes for exploring for metabolites that mediate behavior of other organisms (Bills et al., 2013) and for enzymes that degrade plant polymers (Peterson et al., 2011; van Erven et al., 2020).

During our efforts to identify fungal-produced antifungal metabolites active against the pathogenic yeast *C. neoformans*, we have identified a pair of new 24-carbon macrolides bearing a distinctive phosphoethanolamine substituent (**1** and **2**) and a previously described dimeric epipolythiodioxopiperazine (ETP), leptosin C (**3**), from coprophilous strains of *Preussia typharum* (Dothideomycetes, Sporormiaceae). These compounds (Fig. 1) exhibit selective antifungal activity toward *C. neoformans* compared to *C. albicans*. *Preussia* is an ascomycete genus with a cosmopolitan distribution, and the species are primarily associated with herbivore dung, although they can also be recovered from soil, living plants, and plant litter (Ahmed & Cain, 1972; Doveri, 2004; Furuya & Udagawa, 1972; Gonzalez-Menendez et al., 2017; Mapperson et al., 2014). Frequent previous reports indicate that *Preussia* species are rich sources of bioactive natural products (Bergstrom et al., 1995; Chen et al., 2009, 2020; Du et al., 2012, 2014; Gonzalez-Menendez et al., 2017; Noumeur et al., 2017; Poch & Gloer, 1991; Rangel-Grimaldo et al., 2017; Talontsi et al., 2014; Weber et al., 1990; Weber & Gloer, 1988, 1991; Xu et al., 2019; Zhang et al., 2012). However, to the best of our knowledge, no studies have yet associated secondary metabolites produced by any *Preussia* strain with its respective biosynthetic gene clusters (BGCs). Herein we describe the morphology and phylogenetic placement of the producing fungal strains identified as *P. typharum*, along with their fermentation, isolation, and the structure elucidation, and biological activity of the antifungal molecules. Furthermore, we identify the putative BGCs responsible for the macrolide and ETP assembly from draft genome sequences.

Materials and Methods

General Experimental Procedures

Extracts were fractionated on a Grace Reveleris X2 flash chromatography system equipped with UV and ELSD detectors.

HPLC–DAD–MS analysis employed an Agilent 1260 LC coupled to an Agilent 6120 single quadrupole MS with 0.1% aqueous acetonitrile (A) and 0.1% aqueous formic acid (B) as mobile phases. Chromatographic profiles were monitored by scanning from 190 to 400 nm, and by positive and negative ESI (electrospray ionization)–MS from m/z 160–1500. NMR data were collected at 298 K on a Bruker 500-MHz NMR instrument equipped with a 5-mm triple resonance cryoprobe, with CD_3OD as solvent and tetramethylsilane used as internal standard ($TMS \delta_H$ 0).

Fungal Strains and Fermentation

Strains TTI-0926 and TTI-0947 were recovered from pony dung collected near Fayetteville, Washington Co., Arkansas, USA by use of the particle filtration method (Torres et al., 2011). Strains TTI-1095 and TTI-1099 were isolated from white-tailed deer dung collected in Belington, Barbour Co., West Virginia, USA. Strain TTI-1095 was isolated by use of the ethanol-pasteurization method (Bills et al., 2004; Bills & Polishook, 1993), while strain TTI-1099 was recovered by the particle filtration method. One representative strain from each location was deposited at the USDA Northern Regional Research Laboratory (NRRL) Culture Collection (NRRL 66960 = TTI-0947, NRRL 66961 = TTI-1095).

To grow seed cultures, six agar discs from 2-week old YM agar (malt extract 10 g, yeast extract 2 g, agar 20 g, 1 000-ml deionized H_2O) cultures were inoculated into SMY (maltose 40 g, neopeptone 10 g, yeast extract 10 g, 1 000-ml deionized H_2O) with 0.4% agar in 50-ml aliquots in a 250-ml flask. Seed cultures were grown at 24°C, 220 rpm for 4 days. For the production cultures, 1-ml aliquots of the seed growth were transferred to 50-ml glass vials with 12 ml of media. *Preussia* strains were grown on five media in 12-ml fermentations each. TTI-0926 was grown in Wheat 1 medium (5.0-g whole wheat seeds, 8.5 ml of base liquid consisting of yeast extract 2.0 g, sodium tartrate 10.0 g, KH_2PO_4 1.0 g, $MgSO_4 \cdot 7H_2O$ 1.0 g, $FeSO_4 \cdot 7H_2O$ 0.050 g, 1 000-ml deionized H_2O), CYS80 (sucrose 80 g, yellow cornmeal 50.0 g, yeast extract 1.0 g in 1 000-ml deionized H_2O), MMK2 [mannitol 40 g, yeast extract 5.0 g, Murashige & Skoog Salts (Sigma–Aldrich M-5524) 4.3 g, in 1 000-ml deionized H_2O], Supermalt (malt extract 50 g, yeast extract 10.0 g, $FeSO_4 \cdot 7H_2O$ 0.02 g, $ZnSO_4 \cdot 7H_2O$ 0.007 g, in 1 000-ml deionized H_2O), and MPP [maltose 25 g, glucose 10 g, dried baker's yeast 5.0 g, Pharmamedia (Archer Daniels Midland) 10 g, in 1 000-ml deionized H_2O]. For strain TTI-0947, CYS80 media was substituted for CLA (5.0 g yeast autolysate, 40 g yellow corn meal, 40.0 lactose in 1 000-ml deionized H_2O), Supermalt was substituted for YES (150-g sucrose, 20-g yeast extract, 0.5-g $MgSO_4 \cdot 7H_2O$, 0.010-g $ZnSO_4 \cdot 7H_2O$, 0.005-g

CuSO₄ · 5H₂O in 1 000-ml deionized H₂O) and MPP was replaced for GS [glucose 25 g, corn starch 10.0 g, blackstrap molasses (Brer Rabbit) 5.0 g, casein hydrolysate 4.0 g, meat peptone 1.0 g, 1 000-ml deionized H₂O]. TTI-1095 and TTI-1099 were grown in the same media as TTI-0947, except that GS medium was replaced by GLX medium (10.0-g peptone, 21.0-g malt extract, 40.0-g glycerol, 1.0-g carboxymethyl cellulose in 1 000-ml deionized H₂O). Cultures on the Wheat1, CYS80, and CLA media were incubated statically with vials slanted at a 45° angle; cultures on other media were agitated at 220 rpm.

Genome Sequencing and Annotation of Putative Preussolide and Leptosin Gene Clusters

Strains TTI-0926, TTI-0947, TTI-1095 and TTI-1099 were grown in a static culture of 100-ml SMY for 14 days at 23°C. Mycelium was filtered, pressed dry, frozen at -80°C, and lyophilized. Genomic DNA was purified from ground mycelial powder with a Zymo Research Corporation Quick-DNA™ Fungal/Bacterial Miniprep Kit. For preparation of sequencing libraries, 500 ng of total genomic DNA were used as the template and processed using the KAPA HyperPlus Kit for PCR-free workflows (Roche, Switzerland) according to the manufacturer's instructions. Sequencing libraries were size selected for 600–800-bp fragments using a LightBench (Coastal Genomics, Canada). Whole genomes were sequenced on a HiSeq 4000 Sequencing System (Illumina, USA). The genome was assembled by SPAdes using standard parameters (Bankevich et al., 2012).

The putative preussolide (GenBank MW147207) and leptosin C (GenBank MW161056) gene clusters in TTI-0926 and TTI-1095 were predicted by submitting the unannotated scaffold sequences for antiSMASH analysis (<https://fungismash.secondarymetabolites.org/>) (Blin et al., 2019). The ORFs of the BGCs were further refined by a combination of gene predictions from Augustus (Stanke et al., 2006) and FGENESH (Solovyev et al., 2006) using *Preussia* sp. as the reference genome followed by manual correction of ORFs. Possible functions of predicted hypothetical proteins were explored by analysis of catalytic domains at the Protein Data Bank (<https://www.rcsb.org/>). Reciprocal BLAST searches of predicted proteins and annotated scaffolds with sequences from previously determined core genes of the *akml* cluster BGC (Morishita et al., 2020) from *Aspergillus luchuensis* (= *Aspergillus kawachii*) IFO 4308 (GenBank BACL01000000), the *ciml* BGC (Morishita et al., 2020) from *Colletotrichum incanum* MAFF 238704 (GenBank LFIW00000000), the verticillin BGC (Wang, Hu, et al., 2017) from *Clonostachys rogersoniana* (GenBank KY359203), and the chaetocin BGC (Gerken & Walsh, 2013) from *Collariella virescens* (GenBank KF496217). Orthologous BGCs from TTI-0926, TTI-1095, *A. luchuensis*, *C. incanum*, *C. rogersoniana*, and *C. virescens* were aligned using Easyfig (Sullivan et al., 2011) and plotted to illustrate gene identity between orthologs (%) and their comparative microsynteny.

Phylogenetic Tree Construction

To reconstruct the approximate phylogenetic position of strains TTI-0926, TTI-0947, TTI-1095, and TTI-1099, genomic DNA was purified from lyophilized mycelial powder of strains TTI-0926 and TTI-0947 with a Zymo Research Corporation Quick-DNA™ Fungal/Bacterial Miniprep Kit. The rDNA region containing the internal transcribed spacer (ITS) region with primers ITS1 and ITS5. PCR products were amplified from 30-μl reaction mixtures containing 1.0-μl DNA template, 1.0-μl each forward and reverse primers, 15 μl of 2 × MasterMix (Promega), and 12 μl of H₂O. The PCR parameters were 94°C for 40 s, followed by 40 cycles at 54°C

for 60 s, 72°C for 90 s, and a final extension at 72°C for 10 min. Partial sequences obtained from sequencing reactions were assembled with Geneious (version R11. <https://www.geneious.com/>). ITS sequences amplified from TTI-0926 and TTI-0947 (MW256658, MW256659) were used to search genomic assemblies from strains TTI-1095 and TTI-1099 to locate their respective ITS sequences (GenBank MW256656, MW256657).

A phylogenetic tree was constructed based on alignments of the ITS region. The DNA sequences from other *Preussia* species retrieved from GenBank were aligned by using ClustalW implemented in MEGA X (Kumar et al., 2018), and the resulting alignment was manually trimmed. Phylogenies were inferred by the maximum likelihood (ML) method implemented in MEGA X under a Kimura 2-parameter model with gamma distribution of evolutionary rates. Bootstrap supports for tree nodes were calculated using the default options in MEGA X with 1 000 replicates per run.

Screening for Antimicrobial Activity and Identification of Bioactive Compounds

For initial detection of antifungal activity from previously untested fungal strains, extracts from 12-ml fermentations were tested in agar zone of inhibition assays. Each fermentation was extracted by the addition of an equal volume of methyl ethyl ketone (MEK) followed by shaking for 2 hr. The MEK layer was evaporated under vacuum. Residues were dissolved in DMSO at 10× the original culture volume and 10 μl of each DMSO extract was applied to a 4-mm well aspirated from a plate of YM agar (malt extract 10 g, yeast extract 2 g, agar 20 g, in 1 000 ml of deionized H₂O) seeded with an overnight culture of *C. albicans* ATCC 10231 or *C. neoformans* H99. Plates were incubated at 25°C and examined after 24–48 hr, and zones of inhibition (ZOIs) were photographed.

The antifungal activity produced by strains was tracked by HPLC microfractionation followed by liquid growth inhibition assay directly in the plates used for fractionation as described previously (Perlatti, Nichols, Lan, et al., 2020). Briefly, the HPLC eluents from an Ace Equivalence C₁₈ 150 × 4.6 mm, 5 μm, 35°C, 10–100% A over 20 min, holding 100% for 4 min, 1.0 ml min⁻¹ were collected with a fraction collector. Aliquots of 250 μl were collected in 96-well plates and vacuum-dried. An overnight culture of *C. neoformans* was diluted to O.D. 0.8 in sterile H₂O and then diluted another 500-fold in YM media. An aliquot of 90 μl was transferred to each well, and the plate incubated for 36 hr, afterwards 10 μl of PrestoBlue (Invitrogen) dye was added and incubated for another 12 hr to differentiate growing versus non-growing wells. Antifungal compounds were traced to wells where growth of *C. neoformans* was completely inhibited.

Isolation and Purification of Antifungal Compounds

Strain TTI-1095 was selected for scale-up and was grown in 20 × 250-ml baffled flasks containing 50 ml of MMK2 medium. A 2.5-ml aliquot of a 4-day seed culture in SMY was transferred to each flask and incubated at 23°C and 220 rpm. After 14 days of growth, the whole cultures were extracted by adding 50 ml of MEK to each flask, followed by agitation for 3 hr at 220 rpm. The organic phase was separated, filtered, and evaporated to dryness. The resulting crude extract was dissolved in MeOH:H₂O 9:1, and extracted with hexane. The methanolic fraction was dried, adsorbed in C18 and submitted to flash chromatography (Reveleris C₁₈ RP 40-g cartridge; 20% MeOH for 2 min, 20–40% MeOH in 2 min, held for 1 min, 40–60% MeOH in 2 min, held for 2 min, 60–90% MeOH in 3 min, held for 1.5 min, 90–100% MeOH in 1 min and held for

Table 1 ^1H and ^{13}C NMR Data for **1** and **2** (CD_3OD ; 500 and 125 MHz for ^1H and ^{13}C , Respectively)

Position	1		2	
	δ_{C} , mult	δ_{H} , mult (J in Hz)	δ_{C} , mult	δ_{H} , mult (J in Hz)
1	170.2, C	–	169.8, C	–
2	91.4, CH	5.30, br s	91.5, CH	5.27, br s
3	176.1, C	–	176.3, C	–
4	38.5, CH_2	Ha: 3.58, d, (19) Hb: 3.22, ddd (19, 6.4, 1.4)	38.5, CH_2	Ha: 3.55, d, (19) Hb: 3.06, dd, (19, 5.8)
5	75.7, CH	5.02, t (6.4)	75.7, CH	5.01, dd (6.5, 5.8)
6	93.3, CH	4.3, d (9.3)	93.3, CH	4.29, d (9.4)
7	69.5, CH	3.26, td (9.3, 1.2)	68.7, CH	3.11, ddd (116, 9.4, 1.2)
8	41.5, CH_2	Ha: 1.89, ddd (139, 7.5, 1.2) Hb: 1.55, m	42.7, CH_2	Ha: 1.81, ddd (13, 11, 1.2) Hb: 1.68, ddd (13, 11, 3.8)
9	69.9, CH	3.83, dt (13, 5.3)	71.1, CH	4.21, ddd (11, 8.0, 3.8)
10	36.8, CH_2	1.44, m	133.3, CH	5.32, m
11	25.2, CH_2	1.34, m	134.1, CH	5.65, dt (15, 6.7)
12	30.7, CH_2	1.26, m	32.7, CH_2	2.03, m
13	30.5, CH_2	1.27, m	30.4, CH_2	1.30, m
14	29.4, CH_2	1.25, m	29.4, CH_2	1.25, m
15	30.6, CH_2	1.29, m	30.5, CH_2	1.29, m
16	30.1, CH_2	1.33, m	30.2, CH_2	1.34, m
17	33.2, CH_2	1.98, m	33.4, CH_2	1.98, m
18	131.6, CH	5.35, m	131.4, CH	5.35, m
19	131.8, CH	5.36, m	131.9, CH	5.36, m
20	33.0, CH_2	1.93, m	33.2, CH_2	1.92, m
21	27.0, CH_2	1.35, m	26.6, CH_2	1.37, m
22	36.8, CH_2	Ha: 1.58, m Hb: 1.48, m	36.6, CH_2	Ha: 1.59, m Hb: 1.46, m
23	70.8, CH	4.88, m	70.4, CH	4.93, m
24	20.7, CH_3	1.19, d (6.2)	20.6, CH_3	1.18, d (6.2)
25	62.9, CH_2	4.04, m	63.0, CH_2	4.03, m
26	41.6, CH_2	3.17, m	41.7, CH_2	3.15, m

5 min at a flow rate of 40 ml min^{-1} , with 25 fractions collected. Fractions 20–22 containing active compounds were identified by LC–MS using the same HPLC microfractionation method, pooled, and dried. The enriched fraction was dissolved in MeOH, filtered with a $0.22\text{-}\mu\text{m}$ hydrophilic PTFE syringe filter and further purified by semi-preparative HPLC (Zorbax SB-C₁₈ column $9.4 \times 250 \text{ mm}$, $5 \mu\text{m}$, 30°C ; gradient elution from 45 to 85% of A over 16 min, at 3.5 ml min^{-1}), yielding **1** (t_{R} 7.8 min, 16.8 mg), **2** (t_{R} 6.2 min, 1.7 mg), and **3** (t_{R} 13.2 min, 6.5 mg).

Preussolide A (1): Light brown powder, $[\alpha]_{\text{D}} -64$ (c 0.0025, MeOH); UV (MeOH) λ_{max} (log ϵ); λ_{max} (log ϵ) 242 (4.2); NMR data (CD_3OD) (Table 1). Positive ion HRESIMS m/z 548.2896 $[\text{M} + \text{H}]^+$, (calcd for $[\text{C}_{26}\text{H}_{46}\text{NO}_9\text{P} + \text{H}]^+$, m/z 548.2988).

Preussolide B (2): Light brown powder, $[\alpha]_{\text{D}} -36$ (c 0.00067; MeOH); UV (MeOH) λ_{max} (log ϵ) 242 nm: (3.8); NMR data (CD_3OD) (Table 1). Positive ion HRESIMS m/z 568.2642 $[\text{M} + \text{Na}]^+$ (calcd for $[\text{C}_{26}\text{H}_{44}\text{NO}_9\text{P} + \text{Na}]^+$, m/z 566.2646); negative ion HRESIMS m/z 544.2686 (calcd for $[\text{C}_{26}\text{H}_{44}\text{NO}_9\text{P H}]^-$, m/z 544.2670).

Leptosin C (3): White powder, selected data consistent was with literature values (Du et al., 2014; Takahashi et al., 1994), that is, $[\alpha]_{\text{D}} + 230$ (c 0.0026; MeOH); UV (MeOH) 208 (ϵ 36 000), 301 (ϵ 4 400); ^1H NMR (Supplementary Fig. S18), HRESIMS m/z 741.1273 $[\text{M} + \text{H}]^+$ (calcd for $[\text{C}_{32}\text{H}_{32}\text{N}_6\text{O}_7\text{S}_4 + \text{H}]^+$, m/z 741.1294).

Minimum Inhibitory Concentration

To quantify the inhibitory concentrations of compounds **1–3** for strains of fungal and bacterial pathogens, minimum inhibitory

concentrations (MICs) were measured using species-specific modifications to standard CLSI testing methods (Alexander, 2017). Strains tested included *Staphylococcus aureus* ATCC 43300, *C. albicans* ATCC 10231, *A. fumigatus* AF239, and *C. neoformans* H99, with the latter tested at both 23 and 37°C . Briefly, overnight cultures were sequentially diluted to O.D. 600 of 0.8 in phosphate buffered saline and again by 1 000 \times fold in RPMI-1640 buffered with MOPS (Sigma-Aldrich). The final cell suspension was incubated with serial dilutions of selected compounds dosed at range of $0.5\text{--}256 \mu\text{g ml}^{-1}$ for preussolides and $0.03125\text{--}32 \mu\text{g ml}^{-1}$ for leptosin C. Growth was assessed by adding 10% alamarBlue (Bio-Rad) followed by incubation for 24 hr (*S. aureus*) or 48 hr (*C. albicans*, *A. fumigatus*, and *C. neoformans*).

Macrophage Cytotoxicity Assay

The cytotoxicity of compounds against the macrophage-like murine cell line J774A.1 was evaluated as described previously (Perlatti, Nichols, Alspaugh, et al., 2020). Macrophage J774.1 cells were grown in Dulbecco's Modified Eagle's Medium (DMEM) to 70% confluency, harvested, transferred to 96-well tissue culture plates at 10^5 cells well^{-1} , and incubated overnight at 37°C and 5% CO_2 . Compounds **1** and **3** were added to the DMEM medium in serial twofold dilutions to achieve a dose range of $0.03125\text{--}32 \mu\text{g ml}^{-1}$. The macrophage medium was replaced with the DMEM medium containing compound and incubated for 24 hr at 37°C and 5% CO_2 . Macrophage viability was assessed by the addition of 10% alamarBlue and incubating for 3 hr at 37°C and 5% CO_2 prior to fluorescence measurement (BMG FLUORStar Optima plate reader).

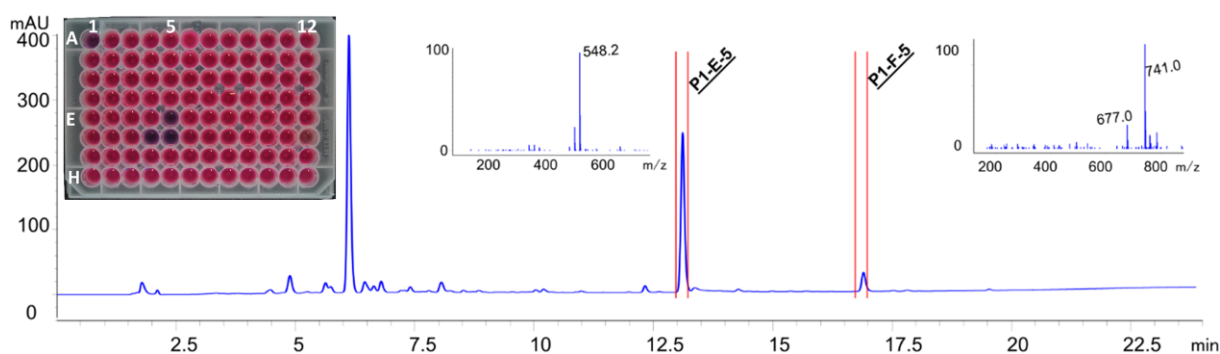


Fig. 2 HPLC microfractionation of extract from strain TTI-1095 grown in MMK2 medium, highlighting the two active peaks associated with growth inhibition of *C. neoformans* at 37°C (upper left, blue wells). ESI⁺-MS spectra for wells E5 and F5 are illustrated in the upper insets.

Results and Discussion

Identification of Strains

The four strains producing compounds **1–3** were judged to be conspecific based on multiple criteria. All four strains were recovered from animal dung, TTI-0926 and TTI-0947 from pony dung from Arkansas, and TTI-1095 and TTI-1099 from white-tailed deer dung from West Virginia. Fermentation extracts of these strains yielded similar patterns of antifungal and antibacterial activity (Fig. 2). HPLC–UV–MS analysis of these extracts indicated that they shared some major metabolites. Mycelial growth and pigments observed among cultures on a set of four different media indicated the strains were highly similar (Supplementary Fig. S1). Sporulation was more or less consistent among the strains, with strains, TTI-0926, TTI-947, and TTI-01099 (Supplementary Figs. S2–S4) producing both membranaceous pycnidia (often referred to as spermagonia (Cain, 1961)) bearing minute, hyaline, globose conidia (Supplementary Fig. S3) and ascomata with four-celled melanized ascospores typical of the genus *Preussia* (Supplementary Figs. S2–S4). Strain TTI-1095 only produced the pycnidial state and never produced fertile ascomata (not shown).

Alignment of the rDNA ITS region of the four strains indicated sequences were 99–100% similar. BLAST searches of public databases with the ITS sequences of all four strains retrieved many sequences with >98% similarity. The majority of the assigned names were associated with the *P. funiculata* clade of the genus *Preussia* (Kruys & Wedin, 2009), including *P. funiculata*, *P. aemulans*, *P. vulgaris*, *P. typharum*, and *P. fleischhakii*, but no coherent pattern with respect to the nomenclature of these strains could be inferred.

To understand the relationships of these four coprophilous strains more precisely, we aligned ITS sequences from strains in and near the *P. funiculata* group and built a phylogenetic tree using the ML method (Supplementary Fig. S5). Our strains fell into a clade with large number of sequences that again corresponded to the *P. funiculata* group (Kruys & Wedin, 2009), and this clade has been observed in other surveys of environmental isolates of *Preussia* species (Gonzalez-Menendez et al., 2017; Massimo et al., 2015). Notably, this clade also included the ITS sequence (GenBank JX143871) from a soilborne strain from Oklahoma, USA designated as *P. typharum* that produced leptosin C (Supplementary Fig. S5) (Du et al., 2014). Therefore, this Oklahoma strain is likely conspecific with our strains. None of the strains included within the terminal clade with our isolates were type strains, and furthermore, living type strains for the core species of the *P. funiculata* clade, *P. funiculata*, *P. aemulans*, *P. vulgaris*, *P. typharum*, are non-existent because they were described during the 19th century (Cain, 1961).

Thus, we were unable to confidently associate rDNA sequences from these strains with those of unambiguously named reference strains. Rather than arbitrarily select a species name, we related morphological features of the strains to authoritative illustrated descriptions from the literature. Diagnostic features included the elongated bases of the asci, four-celled ascospores with transverse septa perpendicular to the longitudinal axis of the spore, each ascospore cell with a longitudinal germ slit, and tapered ascospore terminal cells (Supplementary Figs. S2–S4). The combination of features conformed to the morphological concept of *P. typharum* (Cain, 1961; Doveri, 2004), therefore, we have applied this name to the strains.

Detection of Bioactivity, Isolation, and Characterization of Active Compounds

Organic extracts obtained from strains TTI-0926, TTI-0947, TTI-1095, and TTI-1099 grown in different culture media produced clear inhibitory zones against *S. aureus*, *C. albicans*, and *C. neoformans*. Bioactivity, as assessed by zone sizes, varied with strain, medium, and test pathogen. The largest inhibition zones were observed for *C. neoformans*. HPLC microfractionation guided by liquid *C. neoformans* bioassay at 37°C enabled tracking of the bioactivity to two regions of the chromatogram, where two distinct peaks were observed in wells E5 (r.t. 13.0 min) and F5 (r.t. 16.75 min), respectively (Fig. 2), with similar assay results for the four strains of *P. typharum*.

Strain TTI-1095 was chosen for investigation of the antifungal components because its extracts produced the largest and clearest inhibition zones against *C. neoformans* H99. Scaled-up growth of strain TTI-1095 in MMK2 medium provided adequate material for the purification of compounds **1** and **3**, which corresponded to wells E5 and F5 (Fig. 2), respectively. They were produced in sufficient amounts for detailed characterization, along with a third, minor compound (**2**) with a UV profile similar to that of the peak for **1** observed in well E5.

Purified compound **1** was a light-brown solid. HRMS analysis was consistent with the molecular formula $C_{26}H_{46}NO_9$. A set of 1D (¹H and ¹³C) and 2D (COSY, HSQC, HMBC, and NOESY) NMR data was acquired for **1** in CD₃OD (Supplementary Figs. S6–S11, Table 1). ¹H, ¹³C, and multiplicity-edited HSQC NMR data showed the presence of 26 carbons, of which five are sp²-hybridized, attributed to a carboxyl at δ 169.8, an oxygen-bearing double bond at δ 91.4 and δ 176.3, and another pair of olefinic carbons at δ 131.5 and δ 131.8. The remaining (sp³) carbons were identified as 5 oxymethines, 1 oxymethylene, 1 aminomethylene, 13 other methylenes, and 1 methyl group. COSY cross-peaks allowed the observation of spin-systems corresponding to the H-2-H₂-11 and

H₂-16-H₃-24 units of **1**. Correlations between H₂-12 and H₂-15 were not specifically assigned due to extensive overlap. An HMBC correlation between oxymethine H-23 and C-1 allowed the establishment of the 24-membered macrolide ring. Surprisingly, measurable coupling between H-4a/H-5 and H-5/H-6 was not detected in ¹H NMR, although very weak corresponding correlations were observed in the COSY spectrum. This suggests a dihedral angle close to 90° in each case, and strong NOESY interactions were observed between each of these pairs. HMBC correlations of H-4a (δ 3.58) to C-3, C-5, and C-6, of H-4b (δ 3.22) to C-2 and C-3, of H-5 (δ 5.02) to C-3 and C-6, and of H-6 (δ 4.30) to C-3, C-4, C-5, C-7, and C-8 allowed the establishment of a trisubstituted 3,4,5-trihydrofuran ring bridging C-3 and C-6. This structural unit is rare, and it appears that the only prior report of a metabolite possessing this feature was described in a European patent application that disclosed a compound referred to as SM 140 I discovered from an unidentified *Penicillium* strain (Zeeck et al., 1992). The structure of SM 140 I corresponds well with the gross substructure of **1** from C-1 to C-10, and the relevant ¹H and ¹³C NMR data for **1** match well with those described (Zeeck et al., 1992). A COSY correlation between oxymethylene H₂-25 (δ 4.11) and aminomethylene H₂-26 (δ 3.17) protons indicated the existence of an ethanolamine moiety, insulated from the rest of the molecule as evidenced by the lack of other observable HMBC correlations for their ¹H and ¹³C NMR signals. The doublet signals in the proton-decoupled ¹³C NMR spectrum of **1** for carbons at C-5 (δ_C 75.7, ²J_{CP} = 4.6 Hz) and C-25 (δ_C 62.9, ²J_{CP} = 4.6 Hz), and the adjacent carbons C-4 (δ_C 38.5, ³J_{CP} = 2.9 Hz), C-6 (δ_C 93.6, ³J_{CP} = 5.0 Hz), and C-26 (δ_C 41.6, ³J_{CP} = 5.4 Hz) indicated that the ethanolamine unit is part of a phosphoethanolamine group connected to the macrolide at C-5. The remaining methylenes at C-12–C-15 were set based on the molecular formula, although the corresponding ¹H NMR signals were not precisely located due to extensive overlap. The Z-geometry of the double bond at C-2 was determined based on NOESY correlations between H-2 and H-4a/b. Because the $\Delta\delta_{18,19}$ olefin ¹H NMR signals were overlapped, the corresponding J_{HH} value was not measured, but it was assigned the E geometry on the basis of the δ values of the corresponding allylic carbons (C-17 at δ_C 33.2 and C-20 at δ_C 33.0) and by comparison of these shift values with those of similar compounds (Kozone et al., 2009; Morishita et al., 2020).

The relative configuration of **1** was difficult to assign with confidence by NMR analysis alone due to the flexibility of the macrolide ring. Unfortunately, efforts to crystallize a sample of **1** were unsuccessful. Strong NOESY correlations of H-7 with both H-5 and H-9 suggested an all-cis relative configuration of H-5, H-7 and H-9. The relative configuration of C-6 was proposed as shown based on the absence of NOESY correlations to H-6. These assignments, and proposal of the relative configuration shown at remote stereocenter C-23, would be consistent with those recently elucidated for products of heterologous expression of the *akml* and *ciml* BGCs of *A. luchuensis* and *C. incanum*, respectively (Morishita et al., 2020), and proposed analogy with the corresponding biosynthetic pathway as discussed below. We have named compound **1** as preussolide A. Notably, the presence of a dialkyl phosphoric acid OH group together with a free amine in the molecule indicates that the structure likely exists in the zwitterionic form. The structure shown does not incorporate this feature in order to be consistent with prior reports of this structure type.

Compound **2** exhibited a similar UV profile to that of **1**, and HRMS analysis indicated a formula 2 Da lower than the formula of **1**. The NMR data for **2** (Supplementary Figs. S12–S17, Table 1) indicated a structure similar to that of **1** (Fig. 3). However, the

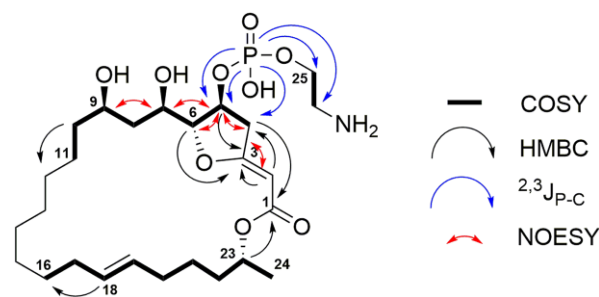


Fig. 3 Main NMR correlations used for the structure elucidation of **1** and **2**.

methylene signals for H₂-10 and H₂-11 observed in the data for **1** were absent, and the signals for H-9 (δ 4.21) and H-12 (δ 2.03) in **2** were deshielded compared to the corresponding signals in the spectrum of **1** (δ 3.83 and δ 1.26 for H-9 and H-12, respectively). Furthermore, new COSY correlations, with H-9 correlating to a hydrogen at δ 5.32 (H-10) and H-12 showing a correlation to δ 5.65 (H-11) indicated the presence of a C-10/C-11 double bond in **2**. In this case, the E-geometry of the double bond at C-10 could be assigned based on the H-10/H-11 J-value (15.2 Hz). All other data acquired aligned well with those of preussolide A. The compound (**2**) was named preussolide B.

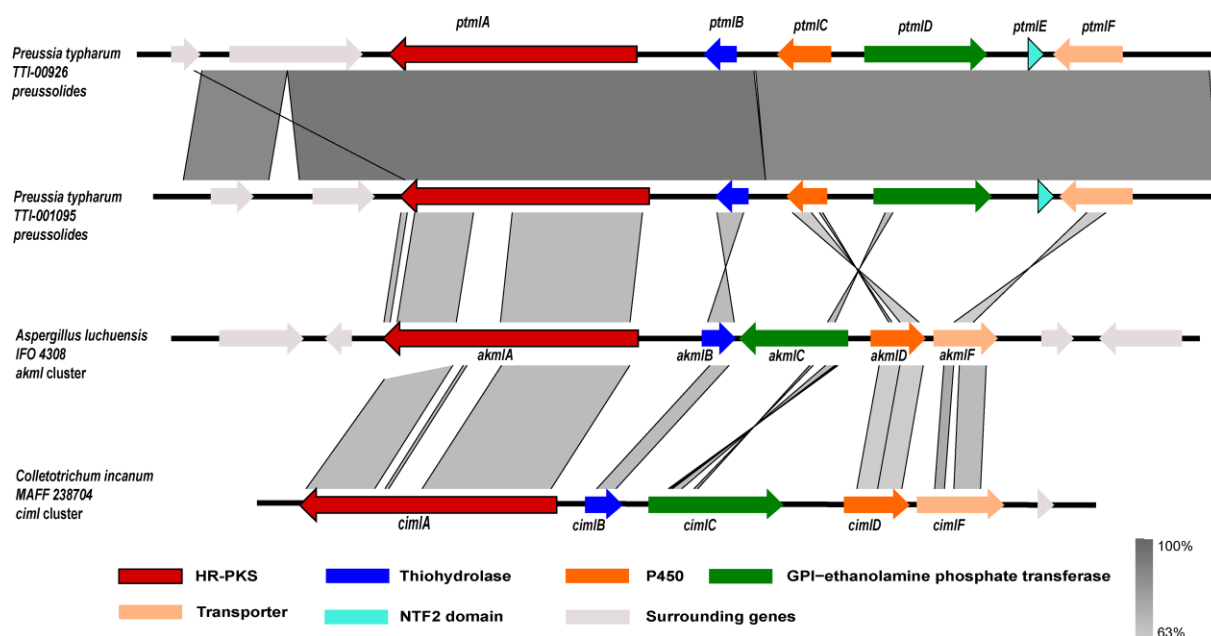
Compound **3** was identified based on its UV, HRMS, [α]_D, and ¹H NMR data (Supplementary Fig. S18) as leptosin C, a cytotoxic dimeric EPT affecting mammalian cells that has been previously reported from strains identified as *Leptosphaeria* sp. (Takahashi et al., 1994; Yanagihara et al., 2005) and *P. typharum* (Du et al., 2014). However, antifungal activity, although predictable based on the structural class, has not previously been reported for leptosin C (Wang, Li, et al., 2017; Yanagihara et al., 2005).

Identification of Gene Clusters Capable of Encoding Biosynthesis of Preussolides and Leptosin

Compounds **1** and **2** belong to a class of natural products known as macrolides that can comprise of macrocyclic lactone rings of varying sizes and a wide range of substituents. Most notably, 14- and 16-membered macrolides produced mainly by actinobacteria have been successfully used as antibacterial, antifungal, immunosuppressive, antiparasitic, and anticancer compounds (Dinos, 2017; Ōmura, 2003; Park et al., 2010; Zuckerman et al., 2011). Fungal macrolides likewise are common and often exhibit potent biological properties (Ackland et al., 1985; Greve et al., 2008; Morishita et al., 2019; Singleton et al., 1958; Stierle et al., 2017; Surup et al., 2018; Xu et al., 2014). Compounds **1** and **2** have a 24-membered macrolactone ring, a structure observed in other classes of molecules such as macrolactins (Gustafson et al., 1989), archazolids (Sasse et al., 2003), patellazoles (Kwan et al., 2012; Zabriskie et al., 1988), lejimalides (Kobayashi et al., 1988), and lecythomycin (Sugijanto et al., 2011). The presence of a phosphoethanolamine moiety or its derivatives is uncommon and only observed thus far in fungi, including eushearilide from *Penicillium shearii* (= *Eupenicillium shearii*) (Hosoe et al., 2006), JBIR-19 and JBIR-20 from *Metarhizium* sp. fE61 (Kozone et al., 2009), and two compounds from *A. luchuensis* IFO 4308 and *C. incanum* MAFF 238704 obtained by heterologous expression of the *akml* and *ciml* BGCs, respectively (Morishita et al., 2020). To the best of our knowledge, this is the first report of a 24-membered macrolide incorporating both a phosphoethanolamine unit and a bridging tetrahydrofuran ring. Bioinformatic triangulation using the *akml* and *ciml*

Table 2 Predicted Proteins of Putative Preussolide Cluster (*ptml*) in *Preussia typharum* and Amino Acid Similarity to *akml* Cluster from *Aspergillus luchuensis*

Gene	Function	Protein ortholog in <i>Aspergillus luchuensis</i>	Similarity %
<i>ptmlA</i>	Polyketide synthase	<i>akmlA</i>	64
<i>ptmlB</i>	Thioesterase	<i>akmlB</i>	55
<i>ptmlC</i>	GPI-ethanolamine transferase	<i>akmlC</i>	41
<i>ptmlD</i>	P450	<i>akmlD</i>	60
<i>ptmlE</i>	NTF2 domain-bearing protein	Absent	–
<i>ptmlF</i>	MFS transporter	<i>akmlF</i>	–

**Fig. 4** Graphic representation of putative and proven macrolide-type gene clusters and their microsynteny. The preussolide (*ptml*) gene cluster from two of the four strains of *Preussia typharum* are illustrated and aligned with the *akml* and *ciml* gene clusters.

gene clusters (Morishita et al., 2020) as probes identified a putative BGC (*ptml*) in all the genomes of the four *P. typharum* strains with high sequence similarities and similar gene content as *akml* and *ciml*. The *ptml* BGG consists of *ptmlA*, a highly reducing polyketide synthase (HR-PKS), a separately encoded thioesterase, *ptmlB*, a P450 *ptmlD*, and a glycosylphosphatidylinositol-ethanolamine phosphate transferase homologue (GPI-EPT) *ptmlC*, that forms the phosphate ester linkage between the phosphoethanolamine group and the macrolide C-5 hydroxyl (Table 2, Fig. 4). Furthermore, in the preussolide, *akml* and *ciml* gene clusters an extra enzyme was evident not mentioned in previous studies (Morishita et al., 2020), a MFS transporter protein encoded by *ptmlF* (Table 2, Fig. 4). Another predicted enzyme, *ptmlE*, absent in the *akml* and *ciml* gene clusters, did not retrieve clear results from protein BLAST. Nonetheless, a search for possible catalytic domains in the Protein Data Bank and alignment of amino acid sequences indicated its distant homology to NTF2 (nuclear transport factor 2)-like enzymes, including AusH (Mori et al., 2017), Trt14 (Matsuda et al., 2015), and PrhC (Matsuda et al., 2016) involved in austinol, terretonin, brevianamide, and paraherquonin biosynthesis, respectively, and BvnE, a semipinacolase participating in the biosynthetic pathway of the indole alkaloid brevianamide (Ye et al., 2020). Despite their seemingly low sequence or functional sim-

ilarity, all these enzymes catalyze the activation of hydroxyl or water molecules and subsequent intramolecular nucleophilic addition. Structural comparison of the putative enzyme product of this gene with those from AusH, Trt14, PrhC, and BvnE revealed a high similarity in their predicted three-dimensional structures (Supplementary Fig. S19).

Based on the structural evidence and the identification of the putative BGC in *P. typharum*, we propose one possible biosynthetic route for the production of **1** and **2**, noting that the timing and sequence of the individual reactions could vary (Fig. 5).

Using the same triangulation approach as above, we were able to identify a putative leptosin C BGC (*ptver*) in all four strains of *P. typharum* that exhibited remarkably similar gene content and order as the previously characterized EPT BGCs encoding the biosynthesis of verticillin and chaetocin (Fig. 6, Table 3).

Antifungal and Cytotoxic Activity of Preussolides and Leptosin C

The results of MIC dilution assays for compounds **1–3** are displayed in Table 4. All three compounds selectively inhibited the growth of *C. neoformans* H99 relative to parallel growth inhibition

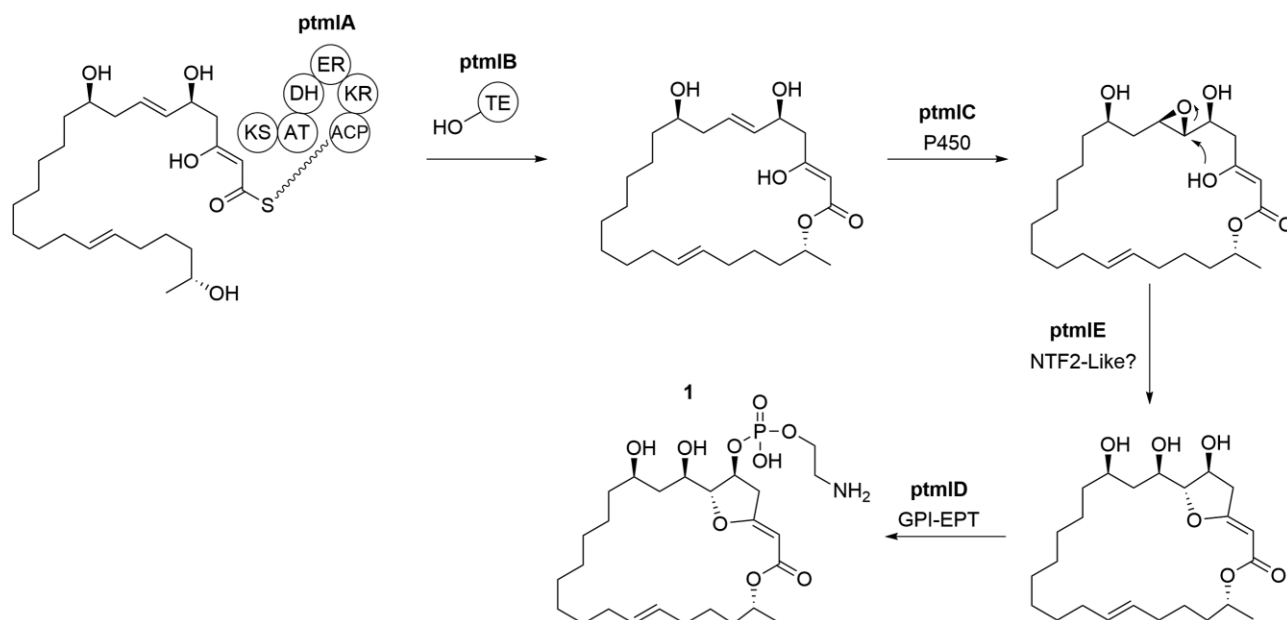


Fig. 5 A possible biosynthetic pathway for preussolides in *Preussia typharum*. Domain structure for the *ptmIA* polyketide is represented graphically.

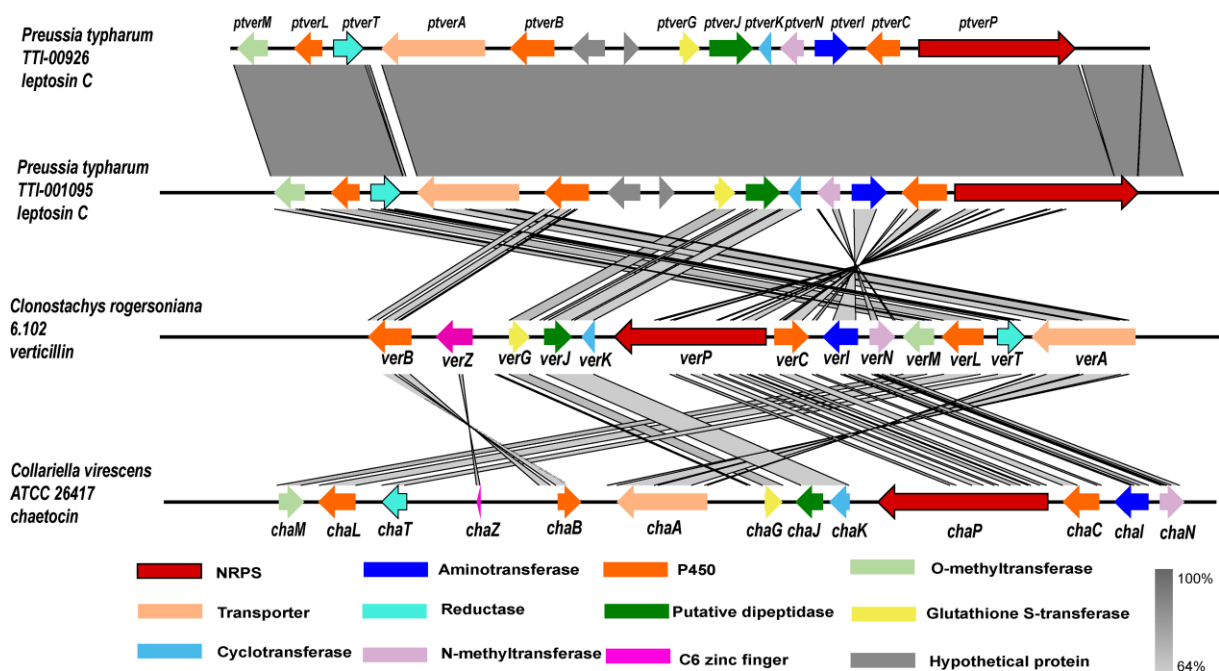


Fig. 6 Graphic representation of putative and proven dimeric epidithiodiketopiperazine gene clusters and their microsynteny. The leptosin C gene cluster (*ptver*) from two of the four strains of *Preussia typharum* are illustrated and aligned with the verticillin (*ver*) and chaetocin (*cha*) gene clusters.

assays with *C. albicans* ATCC 10231. Leptosin C (**3**) was most potent toward *C. neoformans* at 37°C.

Eushearilide, a phosphethanolamine-bearing polyketide, was shown to exhibit qualitative antifungal activity against a broad range of fungi, including pathogenic ascomycetous yeasts, dermatophytes, filamentous ascomycetous, Zygomycetes, and *C. neoformans* (Hosoe et al., 2006). The last three compounds of the *cimIA* pathway produced by heterologous expression (**6–8**) inhibited fungal hyphal growth of *Trichophyton mentagrophytes* IFM 62679 [minimum effective concentration = MEC₈₀ of 6.25 μM (**7**),

12.5 μM (**3**), and 50.0 μM (**4**, **6**, **8**)], and compound **3** also inhibited of *A. fumigatus* IFM 62541 (MEC₈₀ of 25.0 μM) (Morishita et al., 2020). Compounds **3** and **7** inhibited germination of conidia *T. mentagrophytes* IFM 62679 [MIC₉₀ of 12.5 μM (**7**) and 25.0 μM (**3**)] and *A. fumigatus* IFM 62541 [MIC₉₀ of 50.0 μM (**3**, **7**)] (Morishita et al., 2020).

Leptosin C (**3**) was found to selectively inhibit *C. neoformans* in the submicromolar range (Table 4). Other ETPs have also been reported as a selective antifungals against *C. neoformans* when compared to *C. albicans* (Li et al., 2016). Furthermore, leptosin C (**3**), like

Table 3 Predicted Proteins of Putative Leptosin C Cluster (*ptver*) in *Preussia typharum* and Amino Acid Similarity to *ver* Cluster from *Clonostachys rogersoniana*

Gene	Function	Protein homolog in <i>Clonostachys rogersoniana</i>	Similarity %
<i>ptverA</i>	ABC multidrug transporter	<i>verA</i>	64
<i>ptverB</i>	Cytochrome P450	<i>verB</i>	49
<i>ptverC</i>	Cytochrome P450 oxidoreductase	<i>verC</i>	55
<i>ptverG</i>	Glutathione S-transferase	<i>verG</i>	74
<i>ptverI</i>	Aminotransferase	<i>verI</i>	59
<i>ptverJ</i>	Membrane dipeptidase	<i>verJ</i>	71
<i>ptverK</i>	γ -Glutamyl cyclotransferase	<i>verK</i>	68
<i>ptverL</i>	Cytochrome P450	<i>verL</i>	71
<i>ptverM</i>	O-Methyltransferase	<i>verM</i>	67
<i>ptverN</i>	Methyltransferase	<i>verN</i>	58
<i>ptverP</i>	Nonribosomal peptide synthetase	<i>verP</i>	46
<i>ptverT</i>	Oxidoreductase	<i>verT</i>	61
<i>ptverU</i>	Unknown	Hypothetical protein	–
<i>ptverV</i>	Unknown	Hypothetical protein	–
–	C6 zinc finger domain protein	<i>verZ</i>	–

Table 4 Minimum Inhibitory Concentrations (MICs) of 1–3

Organism	Compound (MIC; $\mu\text{g ml}^{-1}$)			
	1	2	3	Control ^a
<i>Staphylococcus aureus</i> ATCC 43300	>256	64	>256	0.05
<i>Candida albicans</i> ATCC 10231	256	256	8	1.56
<i>Cryptococcus neoformans</i> H99 (23°C)	8	32	0.25	0.78
<i>Cryptococcus neoformans</i> H99 (37°C)	4	32	0.06	0.78
<i>Aspergillus fumigatus</i> AF239	8	NT	0.125	
<i>Macrophage</i> J774A.1	32	NT	0.125	

^aChlortetracycline Chlortetracycline + streptomycin were the control for *S. aureus*. Amphotericin B was the control for fungal strains. NT: Not tested.

other dimeric ETPs, exhibited potent mammalian cell cytotoxicity (Table 4).

Summary

In conclusion, by assaying secondary-metabolite-enriched extracts of under-investigated coprophilous ascomycetes (Bills et al., 2013; Bills & Polishook, 1993; Wicklow & Hirschfield, 1979) for growth inhibition of the basidiomycete pathogen, *C. neoformans*, we have identified two new 24-membered phosphoethanolamine-esterified macrolides, preussolides A and B (1, 2), and the ETP dimer, leptosin C (3). In contrast to the recent report on the products of the *akml* and *ciml* BGCs as unexpressed in fungal cultures (Morishita et al., 2020), the preussolide macrolides were readily produced in liquid agitated and solid culture media. They were produced by four coprophilous strains of the *P. funiculata* complex with morphology conforming to *P. typharum*. Additionally, we have identified gene clusters from their draft genome assemblies that likely encode the biosynthesis of 1, 2, and 3. Consequently, this is the first report of a putative secondary metabolite BGCs from strains in the genus *Preussia*. All three compounds showed moderate to potent and selective antifungal activity toward the pathogenic yeast *C. neoformans*.

Supplementary Material

Supplementary material is available online at JIMB (www.academic.oup.com/jimb).

Acknowledgments

This article is dedicated to Prof. Arnold Demain, Merck scientist, industrial microbiologist, and cofounder and instructor of the MIT course in Fermentation Technology. We are grateful to Guy Harris and Steven L. Stephenson for providing dung samples.

Funding

This work was supported by the Kay and Ben Fortson Endowment to G.B., the Chinese Scholarship Council to M.X., and the National Institutes of Health (R01 GM121458).

Conflict of Interest

The sponsors were not involved in the study design; in the collection, analysis and interpretation of data; in the writing of the report; and in the decision to publish the article. All authors declare no conflict of interest. J.E.S. and C.J.B.H. are employees of Hexagon Bio which supported the genome sequencing. This work did not involve studies with human participants or animals.

References

- Ackland, M. J., Hanson, J. R., Hitchcock, P. B., & Ratcliffe, A. H. (1985). Structures of the cephalosporolides B–F, a group of C10 lactones from *Cephalosporium aphidicola*. *Journal of the Chemical Society, Perkin Transactions 1*, 843–847.
- Ahmed, S. I. & Cain, R. F. (1972). Revision of the genera *Sporormia* and *Sporormiella*. *Canadian Journal of Botany*, 50(3), 419–477.
- Alexander, B. D. (2017). Reference method for broth dilution antifungal susceptibility testing of yeasts. *Approved standard M27–A4* (4th ed.) Clinical and Laboratory Standards Institute.
- Bankevich, A., Nurk, S., Antipov, D., Gurevich, A. A., Dvorkin, M., Kulikov, A. S., Lesin, V. M., Nikolenko, S. I., Pham, S., Prjibelski, A. D., Pyshkin, A. V., Sirotkin, A. V., Vyahhi, N., Tesler, G., Alekseyev, M. A., & Pevzner, P. A. (2012). SPAdes: A new genome assembly algorithm and its applications to single-cell sequencing. *Journal of Computational Biology*, 19(5), 455–477.
- Bergstrom, J. D., Dufresne, C., Bills, G. F., Nallin-Omstead, M., & Byrne, K. (1995). Discovery, biosynthesis, and mechanism of action of the

- zaragozic acids: Potent inhibitors of squalene synthase. *Annual Review of Microbiology*, 49(1), 607–639.
- Bills, G. F., Christensen, M., Powell, M., & Thorn, G. (2004). Saprobic soil fungi. In G. Mueller, G. F. Bills, & M. S. Foster (Eds.), *Biodiversity of fungi, inventory and monitoring methods* (pp. 271–302). Elsevier Academic Press.
- Bills, G. F., Gloer, J. B., & An, Z. (2013). Coprophilous fungi: Antibiotic discovery and functions in an underexplored arena of microbial defensive mutualism. *Current Opinion in Microbiology*, 16(5), 549–565.
- Bills, G. F. & Polishook, J. D. (1993). Selective isolation of fungi from dung of *Odocoileus hemionus* (mule deer). *Nova Hedwigia*, 57, 195–206.
- Blin, K., Shaw, S., Steinke, K., Villebro, R., Ziemert, N., Lee, S. Y., Medema, M. H., & Weber, T. (2019). AntiSMASH 5.0: Updates to the secondary metabolite genome mining pipeline. *Nucleic Acids Research*, 47(W1), W81–W87.
- Bongomin, F., Gago, S., Oladele, R. O., & Denning, D. W. (2017). Global and multi-national prevalence of fungal diseases-estimate precision. *Journal of Fungi*, 3(4), 57.
- Brown, G. D., Denning, D. W., Gow, N. A., Levitz, S. M., Netea, M. G., & White, T. C. (2012). Hidden killers: Human fungal infections. *Science Translational Medicine*, 4(165), 165rv13.
- Butts, A., DiDone, L., Koselny, K., Baxter, B. K., Chabrier-Rosello, Y., Wellington, M., & Krysan, D. J. (2013). A repurposing approach identifies off-patent drugs with fungicidal cryptococcal activity, a common structural chemotype, and pharmacological properties relevant to the treatment of cryptococcosis. *Eukaryotic Cell*, 12(2), 278–287.
- Cain, R. F. (1961). Studies of coprophilous ascomycetes VII. *Preussia*. *Canadian Journal of Botany*, 39(7), 1633–1666.
- Chen, H. L., Zhao, W. T., Liu, Q. P., Chen, H. Y., Zhao, W., Yang, D. F., & Yang, X. L. (2020). (+/-)-Preisomide: A new alkaloid featuring a rare naturally occurring tetrahydro-2H-1,2-oxazin skeleton from an endophytic fungus *Preussia isomera* by using OSMAC strategy. *Fitoterapia*, 141, 104475.
- Chen, X., Shi, Q., Lin, G., Guo, S., & Yang, J. (2009). Spirobisnaphthalene analogues from the endophytic fungus *Preussia* sp. *Journal of Natural Products*, 72(9), 1712–1715.
- Dinos, G. P. (2017). The macrolide antibiotic renaissance. *British Journal of Pharmacology*, 174(18), 2967–2983.
- Dix, N. J. & Webster, J. (1995). Coprophilous fungi. In N. J. Dix & J. Webster (Eds.), *Fungal ecology* (pp. 203–224). Springer.
- Doveri, F. (2004). *Fungi Fimicoli Italiani*. Associazione Micologica Bresadola.
- Du, L., King, J. B., Morrow, B. H., Shen, J. K., Miller, A. N., & Cichewicz, R. H. (2012). Diarylcyclopentendione metabolite obtained from a *Preussia typharum* isolate procured using an unconventional cultivation approach. *Journal of Natural Products*, 75(10), 1819–1823.
- Du, L., Robles, A. J., King, J. B., Mooberry, S. L., & Cichewicz, R. H. (2014). Cytotoxic dimeric epipolythiodiketopiperazines from the ascomycetous fungus *Preussia typharum*. *Journal of Antibiotics*, 77(6), 1459–1466.
- Furuya, K. & Udagawa, S. (1972). Coprophilous pyrenomycetes from Japan II. *Journal of General and Applied Microbiology*, 18, 455–467.
- Gerken, T. & Walsh, C. T. (2013). Cloning and sequencing of the chaetocin biosynthetic gene cluster. *Chembiochem*, 14(17), 2256–2258.
- Gonzalez-Menendez, V., Martin, J., Siles, J. A., Gonzalez-Tejero, M. R., Reyes, F., Platas, G., Tormo, J. R., & Genilloud, O. (2017). Biodiversity and chemotaxonomy of *Preussia* isolates from the Iberian Peninsula. *Mycological Progress*, 16(7), 713–728.
- Greve, H., Schupp, P. J., Eguereva, E., Kehraus, S., & Konig, G. M. (2008). Ten-membered lactones from the marine-derived fungus *Curvularia* sp. *Journal of Natural Products*, 71(9), 1651–1653.
- Gustafson, K., Roman, M., & Fenical, W. (1989). The macrolactins, a novel class of antiviral and cytotoxic macrolides from a deep-sea marine bacterium. *Journal of the American Chemical Society*, 111(19), 7519–7524.
- Hosoe, T., Fukushima, K., Takizawa, K., Itabashi, T., Kawahara, N., Vidotto, V., & Kawai, K. (2006). A new antifungal macrolide, eushearilide, isolated from *Eupenicillium shearii*. *Journal of Antibiotics*, 59(9), 597–600.
- Kobayashi, J., Cheng, J., Ohta, T., Nakamura, H., Nozoe, S., Hirata, Y., Ohizumi, Y., & Sasaki, T. (1988). Iejimalides A and B, novel 24-membered macrolides with potent antileukemic activity from the Okinawan tunicate *Eudistoma cf. rigida*. *Journal of Organic Chemistry*, 53(26), 6147–6150.
- Kozone, I., Ueda, J. Y., Watanabe, M., Nogami, S., Nagai, A., Inaba, S., Ohya, Y., Takagi, M., & Shin-ya, K. (2009). Novel 24-membered macrolides, JBIR-19 and -20 isolated from *Metarhizium* sp. fE61. *Journal of Antibiotics*, 62(3), 159–162.
- Kruys, A. & Wedin, M. (2009). Phylogenetic relationships and an assessment of traditionally used taxonomic characters in the Sporormiaceae (Pleosporales, Dothideomycetes, Ascomycota), utilising multi-gene phylogenies. *Systematics and Biodiversity*, 7(4), 465–478.
- Krysan, D. J. (2015). Toward improved anti-cryptococcal drugs: Novel molecules and repurposed drugs. *Fungal Genetics and Biology*, 78, 93–98.
- Kumar, S., Stecher, G., Li, M., Knyaz, C., & Tamura, K. (2018). MEGA X: Molecular evolutionary genetics analysis across computing platforms. *Molecular Biology and Evolution*, 35(6), 1547–1549.
- Kwan, J. C., Donia, M. S., Han, A. W., Hirose, E., Haygood, M. G., & Schmidt, E. W. (2012). Genome streamlining and chemical defense in a coral reef symbiosis. *Proceedings of the National Academy of Sciences of the USA*, 109(50), 20655–20660.
- Li, Y., Yue, Q., Krausert, N. M., An, Z., Gloer, J. B., & Bills, G. F. (2016). Emestrins: Anti-cryptococcus epipolythiodioxopiperazines from *Podospira australis*. *Journal of Natural Products*, 79(9), 2357–2363.
- Mapperson, R. R., Kotiw, M., Davis, R. A., & Dearnaley, J. D. (2014). The diversity and antimicrobial activity of *Preussia* sp. endophytes isolated from Australian dry rainforests. *Current Microbiology*, 68(1), 30–37.
- Massimo, N. C., Nandi Devan, M. M., Arendt, K. R., Wilch, M. H., Riddle, J. M., Furr, S. H., Steen, C., U'Ren, J. M., Sandberg, D. C., & Arnold, A. E. (2015). Fungal endophytes in aboveground tissues of desert plants: Infrequent in culture, but highly diverse and distinctive symbionts. *Microbial Ecology*, 70(1), 61–76.
- Matsuda, Y., Iwabuchi, T., Fujimoto, T., Awakawa, T., Nakashima, Y., Mori, T., Zhang, H., Hayashi, F., & Abe, I. (2016). Discovery of key dioxygenases that diverged the paraherquonin and acetoxydehydroaustin pathways in *Penicillium brasilianum*. *Journal of the American Chemical Society*, 138(38), 12671–12677.
- Matsuda, Y., Iwabuchi, T., Wakimoto, T., Awakawa, T., & Abe, I. (2015). Uncovering the unusual D-ring construction in terretonin biosynthesis by collaboration of a multifunctional cytochrome P450 and a unique isomerase. *Journal of the American Chemical Society*, 137(9), 3393–3401.
- Mori, T., Iwabuchi, T., Hoshino, S., Wang, H., Matsuda, Y., & Abe, I. (2017). Molecular basis for the unusual ring reconstruction in fungal meroterpenoid biogenesis. *Nature Chemical Biology*, 13(10), 1066–1073.
- Morishita, Y., Aoki, Y., Ito, M., Hagiwara, D., Torimaru, K., Morita, D., Kuroda, T., Fukano, H., Hoshino, Y., Suzuki, M., Taniguchi, T., Mori,

- K., & Asai, T. (2020). Genome mining-based discovery of fungal macrolides modified by glycosylphosphatidylinositol (GPI)-ethanolamine phosphate transferase homologues. *Organic Letters*, 22(15), 5876–5879.
- Morishita, Y., Zhang, H., Taniguchi, T., Mori, K., & Asai, T. (2019). The discovery of fungal polyene macrolides via a postgenomic approach reveals a polyketide macrocyclization by *trans*-acting thioesterase in fungi. *Organic Letters*, 21(12), 4788–4792.
- Noumeur, S. R., Helaly, S. E., Jansen, R., Gereke, M., Stradal, T. E. B., Harzallah, D., & Stadler, M. (2017). Preussilides A-F, bicyclic polyketides from the endophytic fungus *Preussia similis* with antiproliferative activity. *Journal of Natural Products*, 80(5), 1531–1540.
- Ōmura, S. (2003). *Macrolide antibiotics: Chemistry, biology, and practice* (2nd ed.). Academic Press. <https://doi.org/10.1016/b978-0-12-526451-8.X5000-0>.
- Park, S. R., Han, A. R., Ban, Y. H., Yoo, Y. J., Kim, E. J., & Yoon, Y. J. (2010). Genetic engineering of macrolide biosynthesis: Past advances, current state, and future prospects. *Applied Microbiology and Biotechnology*, 85(5), 1227–1239.
- Perfect, J. R. (2017). The antifungal pipeline: A reality check. *Nature Reviews Drug Discovery*, 16(9), 603–616.
- Perlatti, B., Nichols, C. B., Alspaugh, J. A., Gloer, J. B., & Bills, G. F. (2020). Sphaerostilbellins, new antimicrobial aminolipopeptide peptaibiotics from *Sphaerostilbella toxica*. *Biomolecules*, 10(10), 1371.
- Perlatti, B., Nichols, C. B., Lan, N., Wiemann, P., Harvey, C. J. B., Alspaugh, J. A., & Bills, G. F. (2020). Identification of the antifungal metabolite chaetoglobosin P from *Discosia rubi* using a *Cryptococcus neoformans* inhibition assay: Insights into mode of action and biosynthesis. *Frontiers in Microbiology*, 11, 1766.
- Peterson, R., Grinyer, J., & Nevalainen, H. (2011). Secretome of the coprophilous fungus *Doratomyces stemonitis* C8, isolated from Koala feces. *Applied and Environmental Microbiology*, 77(11), 3793–3801.
- Poch, G. K. & Gloer, J. B. (1991). Auranticins A and B: Two new depsidones from a mangrove isolate of the fungus *Preussia aurantiaca*. *Journal of Natural Products*, 54(1), 213–217.
- Rajasingham, R., Smith, R. M., Park, B. J., Jarvis, J. N., Govender, N. P., Chiller, T. M., Denning, D. W., Loyse, A., & Boulware, D. R. (2017). Global burden of disease of HIV-associated cryptococcal meningitis: An updated analysis. *The Lancet Infectious Diseases*, 17(8), 873–881.
- Rangel-Grimaldo, M., Rivero-Cruz, I., Madariaga-Mazon, A., Figueroa, M., & Mata, R. (2017). alpha-Glucosidase Inhibitors from *Preussia minimoides*. *Journal of Natural Products*, 80(3), 582–587.
- Richardson, M. J. (2002). The coprophilous succession. *Fungal Diversity*, 10, 101–111.
- Roemer, T., Xu, D., Singh, S. B., Parish, C. A., Harris, G., Wang, H., Davies, J. E., & Bills, G. F. (2011). Confronting the challenges of natural product-based antifungal discovery. *Chemistry & Biology*, 18(2), 148–164.
- Sasse, F., Steinmetz, H., Hofle, G., & Reichenbach, H. (2003). Archazolids, new cytotoxic macrolactones from *Archangium gephyra* (Mycobacteria). Production, isolation, physico-chemical and biological properties. *Journal of Natural Products*, 56(6), 520–525.
- Singleton, V. L., Bohonos, N., & Ullstrup, A. J. (1958). Decumbin, a new compound from a species of *Penicillium*. *Nature*, 181(4615), 1072–1073.
- Solovyev, V., Kosarev, P., Seledsov, I., & Vorobyev, D. (2006). Automatic annotation of eukaryotic genes, pseudogenes and promoters. *Genome Biology*, 7(1), S10.
- Stanke, M., Keller, O., Gunduz, I., Hayes, A., Waack, S., & Morgenstern, B. (2006). AUGUSTUS: Ab initio prediction of alternative transcripts. *Nucleic Acids Research*, 34(Suppl_2), W435–W439.
- Stierle, A. A., Stierle, D. B., Decato, D., Priestley, N. D., Alverson, J. B., Hoody, J., McGrath, K., & Klepacki, D. (2017). The berkeleylactones, antibiotic macrolides from fungal coculture. *Journal of Natural Products*, 80(4), 1150–1160.
- Sugijanto, N. E., Diesel, A., Rateb, M., Pretsch, A., Gogalic, S., Zaini, N. C., Ebel, R., & Indrayanto, G. (2011). Lecythomycin, a new macrolactone glycoside from the endophytic fungus *Lecythophora* sp. *Natural Product Communications*, 6(5), 677–678.
- Sullivan, M. J., Petty, N. K., & Beatson, S. A. (2011). Easyfig: A genome comparison visualizer. *Bioinformatics*, 27(7), 1009–1010.
- Surup, F., Kuhnert, E., Bohm, A., Pendzialek, T., Solga, D., Wiebach, V., Engler, H., Berkessel, A., Stadler, M., & Kalesse, M. (2018). The rickiols: 20-, 22-, and 24-membered macrolides from the ascomycete *Hypoxylon rickii*. *Chemistry*, 24(9), 2200–2213.
- Takahashi, C., Numata, A., Ito, Y., Matsumura, E., Araki, H., Iwaki, H., & Kushida, K. (1994). Leptosins, antitumour metabolites of a fungus isolated from a marine alga. *Journal of the Chemical Society, Perkin Transactions 1*(13), 1859–1864.
- Talontsi, F. M., Lamshoft, M., Douanla-Meli, C., Kouam, S. F., & Spittler, M. (2014). Antiplasmodial and cytotoxic dibenzofurans from *Preussia* sp. harboured in *Enantia chlorantha* Oliv. *Fitoterapia*, 93, 233–238.
- Torres, M. S., Tadych, M., White, J. F., Jr, & Bills, G. F. (2011). Dilution-to-extinction cultivation of endophytic fungi and isolation and detection of grass endophytic fungi in different plant parts, Isolation and identification of fungal endophytes. In S. Sorvari & A. M. Pirttilä (Eds.), *Prospects and applications for plant-associated microbes. A laboratory manual, Part B: Fungi* (pp. 13–18, 153–164). Bio-Bien Innovations.
- van Erven, G., Kleijn, A. F., Patyshakuliyeva, A., Di Falco, M., Tsang, A., de Vries, R. P., van Berkel, W. J. H., & Kabel, M. A. (2020). Evidence for ligninolytic activity of the ascomycete fungus *Podospira anserina*. *Biotechnology for Biofuels*, 13(1), 75. <https://doi.org/10.1186/s13068-020-01713-z>.
- Wang, X., Li, Y., Zhang, X., Lai, D., & Zhou, L. (2017). Structural diversity and biological activities of the cyclodipeptides from fungi. *Molecules (Basel, Switzerland)*, 22(12), 2026. <https://doi.org/10.3390/molecules22122026>.
- Wang, Y., Hu, P., Pan, Y., Zhu, Y., Liu, X., Che, Y., & Liu, G. (2017). Identification and characterization of the verticillin biosynthetic gene cluster in *Clonostachys rogersoniana*. *Fungal Genetics and Biology*, 103, 25–33.
- Weber, H. A., Baenziger, N. C., & Gloer, J. B. (1990). Structure of preussomerin A: An unusual new antifungal metabolite from the coprophilous fungus *Preussia isomera*. *Journal of the American Chemical Society*, 112(18), 6718–6719.
- Weber, H. A. & Gloer, J. B. (1988). Interference competition among natural fungal competitors: An antifungal metabolite from the coprophilous fungus *Preussia fleischhakkii*. *Journal of Natural Products*, 51(5), 879–883.
- Weber, H. A. & Gloer, J. B. (1991). The preussomerins: Novel antifungal metabolites from the coprophilous fungus *Preussia isomera* Cain. *Journal of Organic Chemistry*, 56(14), 4355–4360.
- Wicklow, D. T. (1981). Interference competition and the organization of fungal communities. In D. T. Wicklow & G. C. Carroll (Eds.), *The fungal community* (1st ed., pp. 351–375). Marcel Dekker.
- Wicklow, D. T. (1988). Metabolites in the coevolution of fungal chemical defence systems. In K. A. Pirozynski & D. L. Hawksworth (Eds.), *Coevolution of fungi with plants and animals* (pp. 174–201). Academic Press.
- Wicklow, D. T. (1992). The coprophilous fungal community: An experimental system. In G. C. Carroll & D. T. Wicklow (Eds.), *The*

- fungus community. Its organization and role in the ecosystem* (2nd ed., pp. 715–728). Marcel Dekker, Inc.
- Wicklow, D. T. & Hirschfield, B. J. (1979). Evidence of a competitive hierarchy among coprophilous fungal populations. *Canadian Journal of Microbiology*, 25(7), 855–888.
- Xu, J., Jiang, C. S., Zhang, Z. L., Ma, W. Q., & Guo, Y. W. (2014). Recent progress regarding the bioactivities, biosynthesis and synthesis of naturally occurring resorcinolic macrolides. *Acta Pharmacologica Sinica*, 35(3), 316–330.
- Xu, L. L., Chen, H. L., Hai, P., Gao, Y., Xie, C. D., Yang, X. L., & Abe, I. (2019). (+)- and (–)-Preusolactone A: A pair of caged norsesquiterpenoidal enantiomers with a tricyclo[4.4.0(1,6).0(2,8)]decane carbon skeleton from the endophytic fungus *Preussia isomera*. *Organic Letters*, 21(4), 1078–1081.
- Yanagihara, M., Sasaki-Takahashi, N., Sugahara, T., Yamamoto, S., Shinomi, M., Yamashita, I., Hayashida, M., Yamanoha, B., Numata, A., Yamori, T., & Andoh, T. (2005). Leptosins isolated from marine fungus *Leptosphaeria* species inhibit DNA topoisomerases I and/or II and induce apoptosis by inactivation of Akt/protein kinase B. *Cancer Science*, 96(11), 816–824.
- Ye, Y., Du, L., Zhang, X., Newmister, S. A., McCauley, M., Alegre-Requena, J. V., Zhang, W., Mu, S., Minami, A., Fraley, A. E., Adrover-Castellano, M. L., Carney, N. A., Shende, V. V., Qi, F., Oikawa, H., Kato, H., Tsukamoto, S., Paton, R. S., & Williams, R. M., ...Li, S. (2020). Fungal-derived brevianamide assembly by a stereoselective semipinacolase. *Nature Catalysis*, 3(6), 497–506.
- Zabriskie, T. M., Mayne, C. L., & Ireland, C. M. (1988). Patellazole C: A novel cytotoxic macrolide from *Lissoclinum patella*. *Journal of the American Chemical Society*, 110(23), 7919–7920.
- Zeeck, A., Philipps, S., Mayer, M., Goehrt, A., Granzer, E., Hammann, P., Kirsch, R., & Thiericke, R. (1992). Decarestrictin and related compounds, process for their preparation from *Penicillium* and their use as bactericides and anticholesteremics (EP 497299 A1).
- Zhang, F., Li, L., Niu, S., Si, Y., Guo, L., Jiang, X., & Che, Y. (2012). A thiopyranochromenone and other chromone derivatives from an endolichenic fungus, *Preussia africana*. *Journal of Natural Products*, 75(2), 230–237.
- Zuckerman, J. M., Qamar, F., & Bono, B. R. (2011). Review of macrolides (azithromycin, clarithromycin), ketolids (telithromycin) and glycylicyclines (tigecycline). *Medical Clinics of North America*, 95(4), 761–791, viii.